Journal of Power Sources 182 (2008) 349–352

Contents lists available at ScienceDirect

Journal of Power Sources

journal homepage: www.elsevier.com/locate/jpowsour

Short communication

Synthesis of single crystalline electro-conductive $Na_{0.44}MnO_2$ nanowires with high aspect ratio for the fast charge–discharge Li ion battery

Eiji Hosono [a], Hirofumi Matsuda [a], Itaru Honma [a], Shinobu Fujihara [b], Masaki Ichihara [c], Haoshen Zhou [a,*]

[a] National Institute of Advanced Industrial Science and Technology, Umezono 1-1-1, Tsukuba 305-8568, Japan
[b] Keio University, 3-14-1 Hiyoshi, Kohoku-ku, Yokohama 223-8522, Japan
[c] Material Design and Characterization Laboratory Institute for Solid State Physics University of Tokyo, 5-1-5 Kashiwanoha, Kashiwa, Chiba 277-8581, Japan

ARTICLE INFO

Article history:
Received 18 February 2008
Received in revised form 25 March 2008
Accepted 26 March 2008
Available online 1 April 2008

Keywords:
$Na_{0.44}MnO_2$
Nanowires
Single crystal
Lithium ion battery

ABSTRACT

We report the fast charge–discharge Li ion battery based on the nanostructural controlled $Na_{0.44}MnO_2$ wires with high aspect ratio. The good fast charge–discharge property is observed because the single crystalline $Na_{0.44}MnO_2$ nanowires have a high electronic conductivity as electrode active materials of lithium ion battery due to the one-dimensional single crystalline nanowire. Moreover, such nanosize structure could reduce the required lithium diffusion length in the active materials to the several tens of nanometer, also reduce the effective specific current density by high surface area, and increase the stability of cycle performance by the one-dimensional single crystalline structure.

1. Introduction

The electrode active materials of lithium ion storage device have been widely studied for the portable electric device and electric vehicle (EV) or hybrid EV (HEV). The manganese oxide as positive electrode active material attracts many researcher's attention because the price of manganese oxide is much lower than that of cobalt oxide [1]. To come into wide use of EV, which needs large amount of active materials, the cost performance is important. Moreover, the most important point for the EV is the fabrication of fast charge–discharge lithium storage devices because the general electrode active material for lithium ion battery is not suitable for fast charge–discharge lithium storage property. Recently, the lithium storage devises with fast charge–discharge (high current density such as over 5–10 $A\,g^{-1}$) properties, which overcome the some existing problems in fast charge–discharge condition based on the nanostructure, such as diffusion, effective current densities, cycle performance, have been reported [2–7].

The manganese oxides with crystal structures such as ramsdellite and layered structure are used for positive electrode for lithium storage devices [8]. However, many manganese oxides are unstable to electrochemical cycling and transform into a spinel structure [8]. $Na_{0.44}MnO_2$ is interesting because the large stabilizing sodium ions prevent the conversion into spinel [8,9]. Some works of electrochemical measurement for lithium ion battery using $Na_{0.44}MnO_2$ are reported [1,9–13]. However, the fast charge–discharge Li ion battery has not been investigated. Although Doeff reports the rate of around 0.5 $A\,g^{-1}$, the higher charge–discharge current density must be required for the fast charge–discharge Li ion battery [1]. Hence, the nanostructural controlled $Na_{0.44}MnO_2$ is fabricated by overcome the existing problems in fast charge–discharge condition to satisfy such industrial needs [2,4].

In this work, we report the fast charge–discharge Li ion battery taking the nanostructural controlled $Na_{0.44}MnO_2$ wires with high aspect ratio as positive electrode, which are synthesis by simple low temperature hydrothermal synthesis. Moreover, this hydrothermal synthesis can be also extended to fabricate $LiMn_2O_4$ [14] and $Li_{0.44}MnO_2$ [15] nanowire. In this work, the $Na_{0.44}MnO_2$ nanowires are directly used for lithium ion battery. The good fast charge–discharge property is observed because the single crystalline $Na_{0.44}MnO_2$ nanowires solve the existing problem of the electronic conductivity due to the high conductivity of the nanowires, that of diffusion by reducing the required lithium diffusion length to the diameter about several tens of nanometer, that of current density by reducing the effective specific current density

* Corresponding author. Tel.: +81 298 61 5795; fax: +81 298 61 5799.
E-mail address: hs.zhou@aist.go.jp (H. Zhou).

0378-7753/$ – see front matter © 2008 Elsevier B.V. All rights reserved.
doi:10.1016/j.jpowsour.2008.03.067

based on a high surface area, and that of cycle performance by large stabilizing single crystalline nanowire structure.

2. Experimental

The commercial Mn_3O_4 powders were dispersed into the NaOH aqueous solution (40 ml, 5 mol dm^{-3}). It was placed in the Teflon-lined autoclave. The autoclave was heated at 205 °C for 4 days. After the hydrothermal treatment, the synthesized $Na_{0.44}MnO_2$ was washed repeatedly by deionized water. The washed $Na_{0.44}MnO_2$ was dried at room temperature in the vacuum condition.

The crystal structure was identified using X-ray diffraction (XRD) analysis with a Bruker axs D8 Advance using Cu Kα radiation. The morphology was observed by a field-emission scanning electron microscopy (FESEM) and high-resolution transmission electron microscopy (HRTEM) using a Carl Zeiss Gemini Supra and a JEOL JEM-2010F, respectively. X-ray photoelectron spectroscopy (XPS) was carried out using Al Kα radiation with a Surface Science Instruments S-probe ESCA Model 2803.

Electrochemical measurements were carried based on a three-electrode set up in the twin beaker cell connected with micro-capillary working as a separator. The fabricated high electro-conductive $Na_{0.44}MnO_2$ nanowires were mixed and ground with 5 wt% Teflon powder and 35 wt% ketjen black (KB). The mixture was spread and pressed on the SUS-304 mesh (100 mesh) as working electrode by hand. The paste was implanted into the gap of mesh. Generally, the thickness of the mesh is around 0.174–0.180 mm. After hand-pressing of the paste, the thickness is around 0.185 mm. So, the maximum electrode thickness is around 0.185 mm because the mesh is just covered by the paste and the gap of the mesh is also filled by the paste. The reference and counter electrode were prepared by spreading and pressing of lithium metals on SUS-304 mesh (100 mesh). A 1 mol dm^{-3} $LiClO_4$ in EC/DEC was used as electrolyte. Cell assembly was carried out in a glove box under an argon atmosphere. The weight in specific capacity (mAh g^{-1}) and current rate (A g^{-1}) is calculated by only active materials.

3. Results and discussion

Fig. 1 shows an XRD pattern (θ–2θ scan) of the synthesized nanowires after low temperature hydrothermal treatment. The diffraction peaks agree with those of $Na_4Mn_9O_{18}$ ($Na_{0.44}MnO_2$)

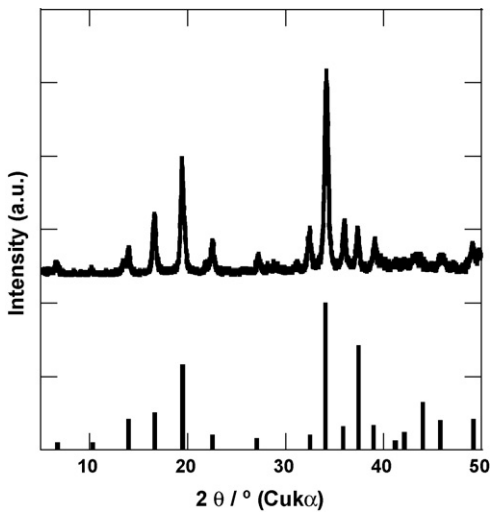

Fig. 1. XRD pattern of the nanowires synthesized by the low temperature hydrothermal treatment. The pattern agrees with the $Na_{0.44}MnO_2$ (JCPDS: 27-0750).

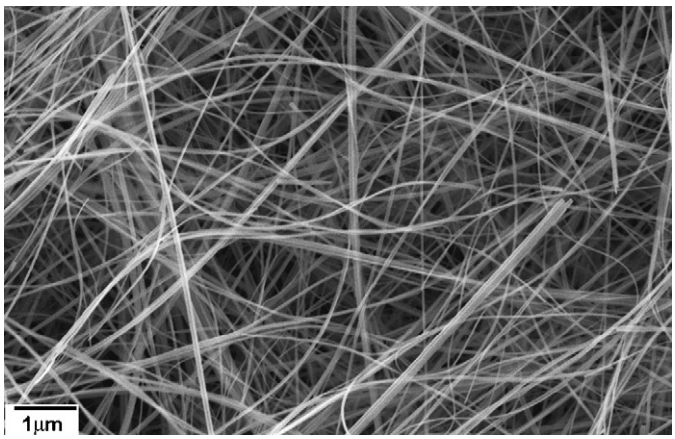

Fig. 2. FE-SEM image of the single crystalline $Na_{0.44}MnO_2$ nanowires.

in the JCPDS No. 27-0750. Fig. 2 is a typical field-emission scanning electron microscope (FE-SEM) image of the synthesized $Na_{0.44}MnO_2$. We can see the nanowires with diameter about the several tens of nanometer. Up to our report [14,15], $Na_{0.44}MnO_2$ wires are fabricated by the solid-state synthesis [16] and high temperature hydrothermal treatment such as 250 °C [17] and 500 °C [18]. However, the wires are assembled by very thick bundle over several 100 μm [16,18]. These bundle structures are not suitable for the fast charge–discharge Li ion battery, which need short lithium diffusion length and large surface area. The homogeneous dispersed nanowires structure of $Na_{0.44}MnO_2$ as shown in Fig. 2 looks suitable for high rate lithium ion battery.

We designed to increase the high electro-conductivity of $Na_{0.44}MnO_2$ nanowires based on this long one-dimensional crystal growth because if many defects exist in the nanowire, the long crystal growth will be impossible and if the nanowires were not defect free, the electro-conductivity along to the growth direction could be improved. In fact, the sheet resistance of the $Na_{0.44}MnO_2$ nanowires, which are pressurized for increasing the density to measure the resistivity, is around 300 kΩ □, which is near to that of transparent conductive ZnO:Al thin film fabricated by sol–gel method [19,20].

The lithium storage characteristics of $Na_{0.44}MnO_2$ nanowires electrode were investigated as shown in Fig. 3. Fig. 3(a) shows the second charge/discharge cycling curves at 0.1, 1.0, 5 and 10 A g^{-1}. In all charge/discharge curves, the shoulders between 2.5 and 3.5 V (Li^+/Li) are observed based on the lithium insertion/extraction and both the discharge and charge processes show similar specific capacities of about 200, 165, 145, and 120 mAh g^{-1} at each current density of 0.1, 1.0, 5.0, and 10 A g^{-1}, respectively. It is the good coulomb efficiency. From this charge/discharge curves, high specific capacities (high energy density) of 120 mAh g^{-1} is observed at very high current density such as 10 A g^{-1}. The 120 mAh g^{-1} is near to the theoretical value of general positive electrode of $LiMn_2O_4$ and $LiCoO_2$ as Eqs. (1) [21] and (2) [21]:

$$2\lambda\text{-}MnO_2 + Li^+ + e = LiMn_2O_4, \text{theoreticalcapacity} : 148\ \text{mAh}\ g^{-1} \quad (1)$$

$$Li_{0.5}CoO_2 + 0.5Li^+ + 0.5e = LiCoO_2, \text{theoreticalcapacity} : 137\ \text{mAh}\ g^{-1} \quad (2)$$

Fig. 3(b) shows the diagram for discharge capacity vs. cycle number for different current density from 0.1 to 10 A g^{-1}. After the 20th cycles, the discharge capacities of the current density at 0.1 and

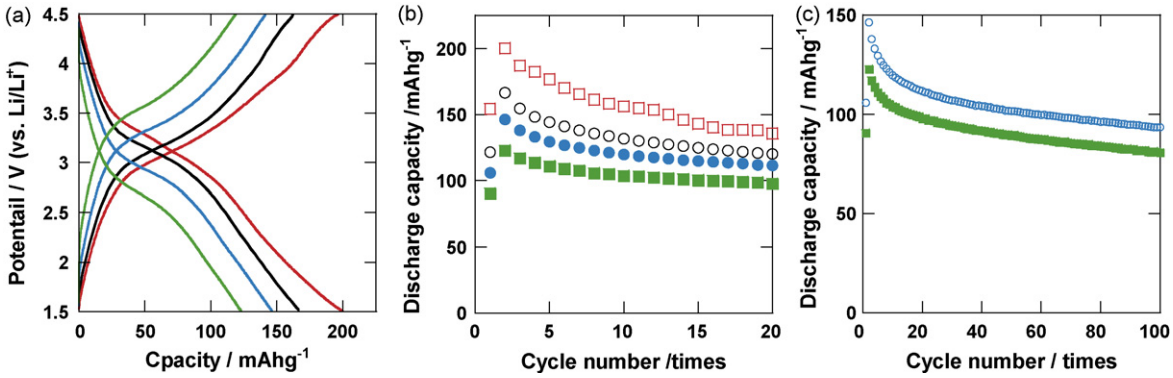

Fig. 3. The lithium storage characteristics of $Na_{0.44}MnO_2$ nanowires electrode. (a) The second cycle charge/discharge curves at various current density (( ) 0.1 A g^{-1}, (—) 1 A g^{-1}, ( ) 5 A g^{-1} and ( ) 10 A g^{-1}). (b) Cycle performance of the $Na_{0.44}MnO_2$ nanowires electrode at various current density up to 20 cycles (( ) 0.1 A g^{-1}, (○) 1 A g^{-1}, (●) 5 A g^{-1} and (■) 10 A g^{-1}). (c) Cycle performance of the $Na_{0.44}MnO_2$ nanowires electrode at the fast charge–discharge lithium storage (high current density) condition up to 100 cycles ((○) 5 A g^{-1} and (■) 10 A g^{-1}).

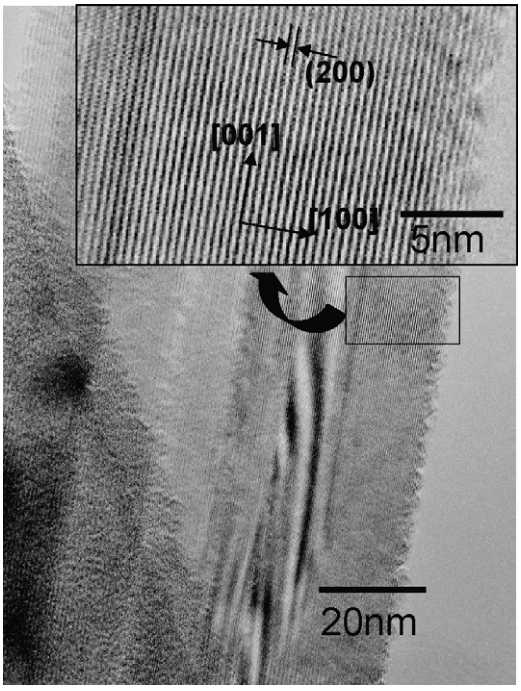

Fig. 4. TEM image of the $Na_{0.44}MnO_2$ nanowires after lithium storage measurement for 100 cycles at fast charge–discharge lithium storage condition of 10 A g^{-1}. The inset is the high-resolution TEM image of the nanowires.

10 A g^{-1} are 120 and 97 mAh g^{-1}, respectively. The capacity of the high current density at 10 A g^{-1} is about 80% of that of low current density at 0.1 A g^{-1} after 20th cycles. In reported works for fast charge–discharge Li ion battery [2–4], the amount of the carbon for conductive assistant materials such as acetylene black and ketjen black is in a range from 45 to 60 wt% [2–4] in the mixture of carbon and Teflon and active materials. In this work, the good fast charge–discharge property is obtained even at the ratio of 35 wt% ketjen black. It is considered that the good high rate property obtained by the high electro-conductivity of the single crystalline $Na_{0.44}MnO_2$ nanowires because the resistivity of single crystalline $Na_{0.44}MnO_2$ nanowires is small as active materials of the metal oxides. Fig. 3(c) shows the diagram for discharge capacity vs. cycle number up to 100 cycles for high current density at 5 and 10 A g^{-1}. After the 100 cycles at even high current density, the capacity is 93 and 80.5 mAh g^{-1} at 5 and 10 A g^{-1}, respectively. These results indicate that electro-conductive $Na_{0.44}MnO_2$ nanowire shows the good fast charge–discharge lithium storage property. Generally, lithium insertion/extraction causes a volume change and collapse of the initial particles due to the change of crystal structure [22]. This volume change makes the cycle performance poor after a number of cycles of charge and discharge process. Fig. 4 shows the TEM image of the $Na_{0.44}MnO_2$ nanowires after the measurement of the lithium storage characteristics at fast charge–discharge condition of 10 A g^{-1} for 100 cycles. The lattice image in inset image shows the clear lattice image. Even after the 100 cycles at 10 A g^{-1}, the single crystalline nanowire nature is maintained. Fig. 5 shows the Li and Na's XPS spectrum of the $Na_{0.44}MnO_2$ nanowires after the 1st dis-

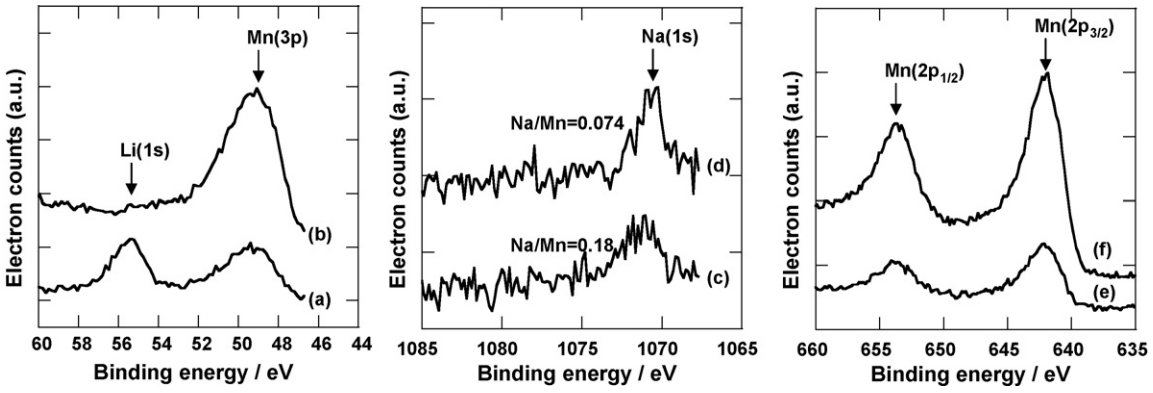

Fig. 5. XPS spectra for the $Na_{0.44}MnO_2$ nanowires. (a, c and e) and (b, d and f) are the spectra of the after the 1st discharge process at 0.1 A g^{-1} and the 5th charge process of discharge–charge cycles at 0.1 A g^{-1} in Li 1s region, Na 1s region, and Mn 2p region, respectively. Na/Mn ratio is calculated by the peaks of Na 1s and Mn $2p_{3/2}$.

charge process and the 5th charge process in the discharge–charge cycles at current density of 0.1 A g^{-1}. Li is detected due to the lithium storage after the 1st discharge process, and then Li cannot be detected after the 5th charge process. It means that the Li is not remained in the electrode after Li extraction. On the other hand, the Na/Mn ratio, which is 0.44 before lithium storage, is decreased to 0.18 at the 1st insertion process and 0.074 at the 5th extraction. The Na is released from the $Na_{0.44}MnO_2$ during the lithium insertion/extraction. The structure of $Na_{0.44}MnO_2$ is a tunnel structure with channel of unusual dimension [8]. It is considered that the release of the Na slightly change the $Na_{0.44}MnO_2$ structure although do not break the tunnel structure by MnO_6 octahedra and MnO_5 square pyramids. This stable crystal structure results in the maintenance of the single crystalline nature even after the lithium insertion/extraction.

4. Conclusions

In summary, we used the $Na_{0.44}MnO_2$ nanowires for the fast charge–discharge lithium storage devices. It indicates good performance by the high electro-conductivity and high stability of the crystal structure, which maintain the single crystalline nature after the lithium insertion/extraction.

References

[1] M.M. Doeff, A. Anapolsky, L. Edman, T.J. Richardson, L.C. De Jonghe, J. Electrochem. Soc. 148 (2001) A230.
[2] T. Kudo, Y. Ikeda, T. Watanabe, M. Hibino, M. Miyayama, H. Abe, K. Kajita, Solid State Ionics 152 (2002) 833.
[3] M. Hibino, H. Kawaoka, H.S. Zhou, I. Honma, Electrochim. Acta 49 (2004) 5209.
[4] H.S. Zhou, D. Li, M. Hibino, I. Honma, Angew. Chem. Int. Ed. 44 (2005) 797.
[5] I. Moriguchi, R. Hidaka, H. Yamada, T. Kudo, H. Murakami, N. Nakashima, Adv. Mater. 18 (2006) 69.
[6] E. Hosono, S. Fujihara, I. Honma, H. Zhou, J. Electrochem. Soc. 153 (2006) A1273.
[7] N. Li, C.R. Martin, J. Electrochem. Soc. 148 (2001) A164.
[8] M.M. Thackery, in: J.O. Besenhard (Ed.), Handbook of Battery Materials, Weily–VCH, 1999, pp. 293–321.
[9] M.M. Doeff, T.J. Richardson, L. Kepley, J. Electrochem. Soc. 143 (1996) 2507.
[10] M.M. Doeff, T.J. Richardson, J. Hollingworth, C.H. Yuan, M. Gonzales, J. Power Sources 112 (2002) 294.
[11] M.M. Doeff, T.J. Richardson, K.T. Hwang, J. Power Sources 135 (2004) 240.
[12] J. Akimoto, J. Awaka, Y. Takahashi, N. Kijima, M. Tabuchi, A. Nakashima, H. Sakaebe, K. Tatsumi, Electrochem. Solid State Lett. 8 (2005) A554.
[13] M. Dollé, S. Patoux, M.M. Doeff, Chem. Mater. 17 (2005) 1036.
[14] E. Hosono, T. Kudo, I. Honma, H.S. Zhou, unpublished work.
[15] E. Hosono, T. Kudo, M. Ichihara, I. Honma, H.S. Zhou, unpublished work.
[16] A. Eftekhari, M. Kazemzad, F. Moztarzadeh, Mater. Res. Bull. 19 (2005) 1229.
[17] Q. Feng, T. Horiuchi, L. Liu, K. Yanagisawa, T. Mitsushio, Chem. Lett. 40 (2000) 2205.
[18] S. Hirano, R. Narita, S. Naka, Mater. Res. Bull. 19 (1984) 1229.
[19] S.Y. Kuo, W.C. Chen, F.I. Lai, C.P. Cheng, H.C. Kuo, S.C. Wang, W.F. Hsieh, J. Cryst. Growth 287 (2006) 78.
[20] S. Fujihara, C. Sasaki, T. Kimura, Key Eng. Mater. 181-1 (2000) 109.
[21] M. Winter, J.O. Besenhard, M.E. Spahr, P. Novák, Adv. Mater. 10 (1998) 725.
[22] H. Kawaoka, M. Hibino, H.S. Zhou, I. Honma, J. Power Sources 125 (2004) 85.